Upper-Air Density and Temperature by the Falling-Sphere Method*

F. L. BARTMAN, L. W. CHANEY,† L. M. JONES, AND V. C. LIU
Engineering Research Institute, University of Michigan, Ann Arbor, Michigan

(Received December 23, 1955)

Upper-atmosphere air densities and temperatures have been calculated from the measured trajectory data of a falling sphere. Densities were calculated from the equation for the drag force on the falling sphere, and temperatures were then obtained by using the hydrostatic equation and the equation of state of a perfect gas. The aerodynamic background and instrumentation are described; the method of calculation and the errors are discussed. The results of four rocket flights which carried the experiment are given. Comparison with the average of other rocket measurements indicates agreement with these results.

I. INTRODUCTION

THE falling-sphere method for the measurement of upper-air density and temperature was developed in the Department of Aeronautical Engineering of the University of Michigan as part of a research program investigating pressure, density, temperature, and composition of the atmosphere to 100 km. It was conceived as a simple alternative to other aerodynamic methods used during the program which required the measurement of pressure-gauge outputs and rocket angle of attack in addition to the measurement of velocity. The sphere results are derived from trajectory measurements only. Further, a sphere has no angle of attack, although it has finally developed that the changing orientation of the internal antenna introduces errors which cannot be corrected for completely.

The method consists of ejecting from a rocket, near the peak of its trajectory, an inflatable nylon sphere 4 feet in diameter. The sphere contains a miniature DOVAP[1,2] (doppler velocity and position) transponder and antenna which, together with the DOVAP ground system, is used to determine the sphere trajectory. From these data and the drag equation, density is calculated. In turn, with the use of the hydrostatic equation and the equation of state of a gas, temperatures are obtained.

II. AERODYNAMICS

The forces acting on a free-falling body, the density of which is large compared to that of the ambient atmosphere, are gravitational attraction and aerodynamic drag. The lateral force induced by spinning is negligible compared to drag in this experiment because the rotational circumferential velocity is negligible compared to the translational velocity. Drag is generally expressed as:

$$D=\tfrac{1}{2}\rho V^2 A C_D, \tag{1}$$

where

ρ = ambient atmospheric density.
V = velocity of the body relative to the atmosphere.
A = maximum cross-sectional area.
C_D = drag coefficient, a dimensionless parameter.

The equation of motion of a free-falling body is

$$\mathbf{g}-\frac{d\mathbf{V}}{dt}=\frac{\rho A C_D}{2m}|\mathbf{V}|\mathbf{V}, \tag{2}$$

where

g = acceleration of gravity.
t = time.
m = mass of body.

Equation (2) is a vector equation which may be resolved into component equations. The relative velocity $\mathbf{V}$ may be resolved into

$$\mathbf{V}=\mathbf{v}-\mathbf{w}, \tag{3}$$

where

$\mathbf{v}$ = velocity of the body relative to the earth.
$\mathbf{w}$ = velocity of wind, which is defined as the local velocity of the atmosphere relative to earth and is assumed steady.

The sphere experiment is designed to measure ambient density ρ in terms of the other parameters in Eq. (2). A amd M are measured before the flight; g is known as a function of altitude[3]:

$$g(h)=g_{\text{sea level}}-0.0003086h,$$

where

g = cm/sec^2.
h = altitude above sea level in meters.

Winds can be measured, in principle, by the sphere experiment. The horizontal component can be obtained from the DOVAP data since three dimensions of the trajectory are obtained. Vertical winds are indistinguishable from a density gradient in the case of a single sphere, but could be solved from the simultaneous

* The research program under which the work was accomplished was carried out in the Department of Aeronautical Engineering under Evans Signal Laboratory Contracts DA-36-039 SC-125, DA-36-039 SC-15443, and 23488-PH-54-92 with the Engineering Research Institute of the University of Michigan. See Progress Reports of these contracts and F. L. Bartman *et. al.*, J. Atmos. Terr. Phys. Spec. Suppl. 1 (1954).

† Present address: Micrometrical Development Corporation, Ann Arbor, Michigan.

[1] E. D. Hoffleit, Sci. Monthly 68, 172 (1949).

[2] L. G. deBey and E. D. Hoffleit, Ballistic Research Laboratories, Report BRL-R-677 (1948).

[3] *International Critical Tables I*, (McGraw-Hill Book Company, Inc., New York, 1926), p. 402.

equations of two spheres of different A/m ratios.[4] However, since the method is not a particularly sensitive one for winds, the wind technique has not been pursued. Also, it can be shown that only minor errors result from neglecting typical winds. Estimated values of typical winds have been given by Bartman, Liu, and Schaefer.[5]

The vertical component of Eq. (2) can be written as

$$\frac{2m}{AC_D v^2 \cos^2\beta}\left|g-\frac{dv}{dt}\cos\beta\right| = \rho\left(1-\frac{2w\cos\alpha}{v\cos\beta}+\frac{w^2\cos^2\alpha}{v^2\cos^2\beta}\right), \quad (4)$$

where α and β are the direction angles to the vertical of the wind and sphere velocity vectors, respectively, provided the horizontal component of the relative air velocity V is negligible compared to its vertical component. If $(w\cos\alpha/v\cos\beta)\ll 1$ (that is, if the vertical wind component is small compared to that of the sphere velocity, $v_h = v\cos\beta$), the wind effect, $2\rho w\cos\alpha/v\cos\beta$, amounts to a first-order correction to ρ.

It can be shown by dimensional analysis[6] that the aerodynamic drag force D on a sphere which moves in a rarefied gas can be expressed as

$$\frac{2D}{\rho v^2 A} = C_D\left(M, \frac{\lambda}{d}\right), \quad (5)$$

where M and λ/d are the dimensionless parameters, Mach number, and Knudsen number, respectively.

M = Mach number $= v/a$.
a = ambient sound velocity.
λ/d = Knudsen number.
λ = mean free path.
d = a characteristic dimension of the body.

Another dimensionless parameter which is commonly used to indicate the relative significance of inertia force to viscous force is Reynolds number, $\mathrm{Re} = v\rho d/\mu$, where μ is the coefficient of viscosity of air. It is known from kinetic theory that μ is proportional to $\rho a\lambda$, which leads to the relation

$$\frac{\lambda}{d} \sim \frac{M}{\mathrm{Re}}.$$

Thus C_D depends on Mach number and Reynolds number. Values of C_D are obtained from ballistic range, wind tunnel, and similar measurements. The values are then used for the large spheres of the experiment at the same values of M and Re.

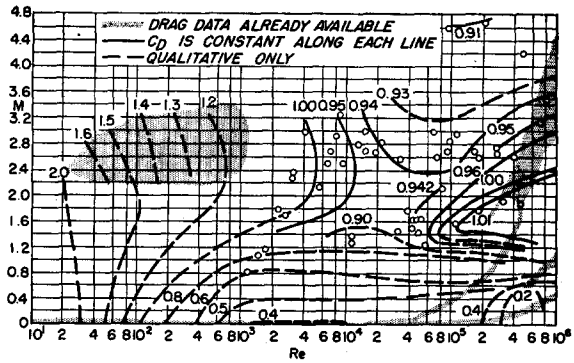

FIG. 1. Sphere drag-coefficient data.

Spheres, because of their geometrical simplicity, are commonly used to calibrate flow devices such as ballistic ranges and wind tunnels. In spite of this, the "map" of C_D as a function of M and Re had significant gaps in the region of interest to the sphere experiment. At the request of the University of Michigan, the Naval Ordnance Laboratory at White Oak, Maryland, undertook to fill in some of the regions of interest. The result is seen in Fig. 1.[7]

In view of the above discussion, the following equation is used in the measurement of density:

$$\rho = \frac{2m}{V^2 AC_D\cos^2\beta}\left|g-\frac{dv}{dt}\cos\beta\right|. \quad (6)$$

The details of the density calculations and the derivative temperature calculations are given in Sec. IV.

III. INSTRUMENTATION

In order to obtain a measurable drag at significant altitudes, the sphere should be light and large and should be dropped from as high an altitude as possible. It must also be large enough to accommodate the DOVAP antenna. On the other hand, it is limited in size by the fact that it must be fitted in the rocket, that it must be possible to construct by available techniques, and must be inflatable with a reasonable amount of gas. Also, it is desirable that the sphere envelope be nonmetallic so that an internal antenna may be used. The four spheres flown differed somewhat in construction and method of ejection. A description of the last instrumentation will illustrate the main features.

The sphere was made[8] of 16 nylon cloth gores, 0.020 in. thick, cut on longitudinal lines, and heat sealed together with lap joints. Two rings, six inches in

[4] V. C. Liu, "On sphere method of ambient temperature measurement in the upper atmosphere with wind," Signal Corps Contract No. DA-35-039 SC-125, Engineering Research Institute, University of Michigan, Tech. Memo. No. 3 (1951).

[5] Bartman, Liu, and Schaefer, "An aerodynamic method of measuring the ambient temperature of air at high altitudes," Signal Corps Contract No. W-36-039 SC-32307 (1950), p. 33.

[6] W. J. Duncan, *Physical Similarity and Dimensional Analysis* (Edward Arnold and Company, London, 1953).

[7] A. May and W. R. Witt, Jr., "Free flight determinations of drag coefficients of spheres," U. S. Naval Ordnance Laboratory, NAVORD Report 2352 (1952).

[8] Manufactured by Goodyear Tire & Rubber Company of Akron, Ohio.

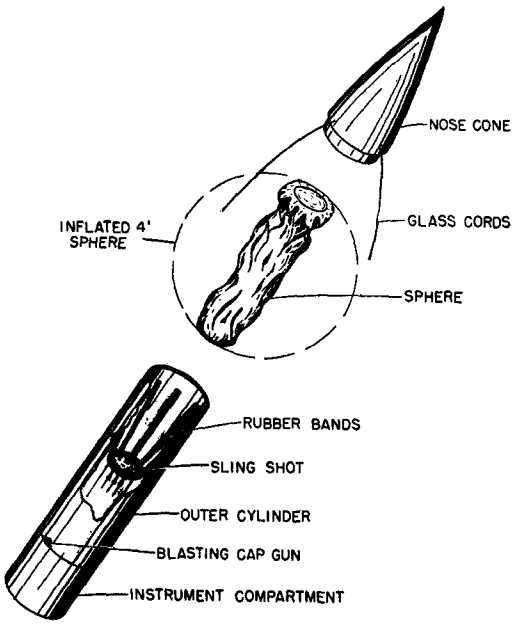

FIG. 2. Sphere rocket instrumentation.

diameter, made of solid nylon were heat sealed to the cloth gores in diametrically opposite positions. These rings accommodated access ports. The internal equipment was located within a 5-in. cylinder approximately 3 ft long, lying along a diameter. More than two thirds of the total length was occupied by a Fiberglas inflation bottle[9] carrying nitrogen at 460 psia. At one end of the bottle was mounted an inflation valve which released the nitrogen from the bottle to the sphere upon ejection of the sphere from the rocket. At the other end of the bottle was mounted the DOVAP transponder, the antenna for which was mounted on the cylinder. Access to the transponder and inflation valve was through the ports mentioned above. The complete sphere was 4 ft in diameter and weighed 20 lb.

In the rocket, the sphere was packed tightly around the inflation bottle within the 15-in. diameter forward section of the Aerobee. This section was made of Textolite to permit operation of the DOVAP during ascent of the rocket. The collapsed sphere rested on a large rubber-band slingshot. The sphere and slingshot were held in the cocked position by the rocket nose cone, which in turn was held down by two longitudinal Fiberglas cords running outside the rocket skin. These passed over blasting cap "guns" which were fired near peak on DOVAP command, thus breaking the cords and permitting the slingshot to eject the nose cone and sphere. The inflated pressure of the sphere was 3 psia, which was sufficient to make it hard and rigid. Figure 2 is a schematic of the sphere ejection system.

The DOVAP system was installed and operated at White Sands Proving Ground (WSPG) by Ballistic Research Laboratories of Aberdeen Proving Ground. It operates as follows: A continuous-wave radio signal of 36.94 Mc is transmitted from a ground transmitter to the sphere. The sphere transponder doubles and retransmits the 73.88-Mc signal to an array of ground receivers. At the receiver stations, the received signal is heterodyned against the transmitter signal which has been received on another receiver directly from the transmitter and doubled. Their difference frequency, which is proportional to the velocity with which the transmitter-sphere-receiver path length is changing, is sent over wire lines to a central recording station. Each doppler cycle represents about 13 ft of distance so that, starting from a known point and counting cycles as a function of time, one can measure the instantaneous transmitter-sphere-receiver distances (u_i). The transmitter-receiver distances are fixed and known. At any given time the sphere lies on the loci of points of the u_i distances. These loci are ellipsoids of revolution, the intersection of three of which uniquely determine the position of the sphere in space. In practice, more than three stations are used to give a statistical and reliability advantage. Also, by using more than one receiver with differently polarized antennae at each station, much can be learned about the spin of the sphere. This is necessary in order to correct for false doppler cycles introduced by the rotation of the antenna.

IV. CALCULATIONS

In this discussion, the coordinates (x_1,x_2,x_3) are those of a right-Cartesian system with origin at the Aerobee launcher and with x_1 east, x_2 north, and x_3 normal upward to the plane of x_1 and x_2. The coordinate x_3 can be converted to altitude above sea level by adding the elevation of the launcher (4000 feet). It is not necessary to consider the earth's curvature and rotation in the calculations.

The data from DOVAP consist of position (x_1,x_2,x_3), velocity $(\dot{x}_1,\dot{x}_2,\dot{x}_3)$, and acceleration $(\ddot{x}_1,\ddot{x}_2,\ddot{x}_3)$ components as functions of time, at half-second intervals.

1. Density Equation

The vector equation of motion of the sphere (2) can be resolved into three components:

$$|g|+\ddot{x}_3=-\frac{\rho AC_D}{2m}(\dot{x}_3-w_3)\times[(\dot{x}_1-w_1)^2+(\dot{x}_2-w_2)^2+(\dot{x}_3-w_3)^2]^{\frac{1}{2}}, \quad (7)$$

$$\ddot{x}_2=-\frac{\rho AC_D}{2m}(\dot{x}_2-w_2)\times[(\dot{x}_1-w_1)^2+(\dot{x}_2-w_2)^2+(\dot{x}_3-w_3)^2]^{\frac{1}{2}}, \quad (8)$$

$$\ddot{x}_1=-\frac{\rho AC_D}{2m}(\dot{x}_1-w_1)\times[(\dot{x}_1-w_1)^2+(\dot{x}_2-w_2)^2+(\dot{x}_3-w_3)^2]^{\frac{1}{2}}, \quad (9)$$

[9] Manufactured by Young Development Company of Rocky Hill, New Jersey.

where w_1, w_2, w_3=east, north, and vertical velocity components of the wind vector relative to the launcher.

Neglecting wind by setting $w_1=w_2=w_3=0$ in Eq. (7), gives

$$\rho=-\frac{2m(|g|+\ddot{x}_3)}{AC_D\dot{x}_3 v}, \tag{10}$$

where

$$v=(\dot{x}_1^2+\dot{x}_2^2+\dot{x}_3^2)^{\frac{1}{2}}; \tag{11}$$

v is the resultant velocity of the sphere relative to the launcher. Equation (10) is used for the density calculations. When the density at a particular altitude $x_3(h)$ is considered, the equation is written as (Fig. 3):

$$\rho(h)=-\frac{2m(|g|+\ddot{x}_3(h))}{AC_D(h)\dot{x}_3(h)v(h)}. \tag{12}$$

2. Temperature Equation

The hydrostatic equation and equation of state of a perfect gas may be written as

$$dp=-g\rho dx_3, \tag{13}$$

$$p=\rho\frac{R}{M_a}T, \tag{14}$$

where

p=ambient pressure.
R=universal gas constant.
M_a=average molecular weight of air.

Integrating Eq. (13), we obtain

$$p(h)=-\int_{x_3(0)}^{x_3(h)} g\rho dx_3+p(0)$$

$$=\int_{x_3(h)}^{x_3(0)} g\rho dx_3+p(0), \tag{15}$$

where

$$p(0)=\rho(0)\frac{R}{M_a}T(0)=\text{pressure at altitude } x_3(0).$$

$$p(h)=\rho(h)\frac{R}{M_a}T(h)=\text{pressure at altitude } x_3(h).$$

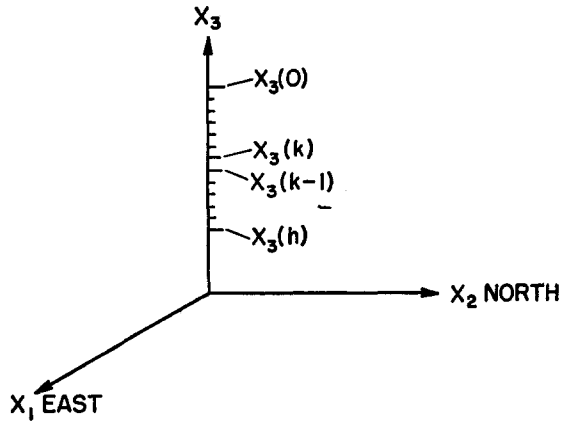

FIG. 3. Coordinate system.

Then,

$$T(h)=-\frac{\int_{x_3(0)}^{x_3(h)} g\rho dx_3}{\rho(h)R/M_a}+\frac{\rho(0)}{\rho(h)}T(0), \tag{16}$$

or

$$T(h)=I(h)+\frac{\rho(0)}{\rho(h)}T(0), \tag{17}$$

where

$$I(h)=-\frac{\int_{x_3(0)}^{x_3(h)} g\rho dx_3}{\rho(h)R/M_a}. \tag{18}$$

Equation (16) can be used to calculate temperature at the altitude $x_3(h)$ from the measured densities in the altitude range $x_3(0)$ to $x_3(h)$, provided $T(0)$ at $x_3(0)$ is known. Since $T(0)$ is not known, a reasonable value is assumed. If the assumed value is in error, $T(h)$ will also be in error. However, since $T(h)$ is the sum of two terms:

$$T(h)=I(h)+\frac{\rho(0)}{\rho(h)}T(0),$$

the error in $T(h)$ caused by the error in $T(0)$ will decrease as the calculation proceeds and $I(h)$ becomes the dominant term. At about 45 000 ft below $x_3(0)$, $I(h)$ is nearly 10 times as large as $\rho(0)T(0)/\rho(h)$, and the error in $T(h)$ due to the error in $T(0)$ becomes negligible.

3. Detailed Procedure

Using values of $\ddot{x}_3$, $\dot{x}_3$, x_3, and v obtained from DOVAP, values of A, m, and d measured before the flight, accepted values of g, C_D, and μ, and assumed curves of ρ, T, and a,[10] a calculation is made at each trajectory data point [each $x(h)$], as follows:

(1) μ is determined from the assumed value of T.
(2) $M=v/a$ and $\mathrm{Re}=\rho vd/\mu$ are calculated.
(3) C_D is read from the chart of C_D as a function of M and Re.
(4) $\rho(h)$ is calculated, using Eq. (12).
(5) $T(h)$ is calculated, using Eq. (17). $I(h)$ in this equation is obtained by numerical integration of the values $\rho(h)$, $g(h)$, using the relation

$$I(h)=\sum_{k=1}^{h}$$

$$\times\frac{[x_3(k)-x_3(k-1)][\rho(k)g(k)-\rho(k-1)g(k-1)]}{\ln\dfrac{\rho(k)g(k)}{\rho(k-1)g(k-1)}}. \tag{19}$$

[10] Averaged internally consistent values of atmospheric constants have been prepared by the Upper Atmosphere Rocket Research Panel (UARRP); see The Rocket Panel, Phys. Rev. 88, 1027–1032 (1952).

TABLE I. Acceleration scatter band widths and probable errors.

	Width of band of scatter in acceleration data	Maximum error in acceleration	Probable error in acceleration
Patton	3 ft/sec²	1.5 ft/sec²	0.5–0.75 ft/sec²
SC-23	8	4	1.2–2.0
SC-29	11	5.5	1.65–2.75
SC-30	8	4	1.2–2.0
SC-31	12	6	1.8–3.0

This formula results from assuming that in a plot of $\rho(h)g(h)$ *vs* h, the values are connected by exponentials. This implies that temperature is constant in the layer $x_3(k)-x_3(k-1)$.

(6) The calculated values of $\rho(h)$ and $T(h)$ will, in general, differ from the assumed values. Steps 1 to 5 are then repeated, using the newly calculated values of $\rho(h)$ and $T(h)$ in place of the assumed values. This process "converges" rapidly, because C_D does not vary rapidly with M and Re, so that usually within one to three tries agreement is reached between the initial and final values of $\rho(h)$ and $T(h)$.

V. ERRORS

The sources of error in the calculated density are: the neglect of winds, and errors in the measurements of $\ddot{x}_3$, $\dot{x}_3$, C_D, m, and A. The last two are negligibly small. The temperatures calculated have additional errors due to errors in $T(0)$ and $I(h)$. The errors from individual sources were estimated and combined by error theory into net errors in density and temperature.

1. Winds

The errors caused by neglecting winds of known velocities can be calculated from Eqs. (7), (8), and (9). Neglecting a vertical wind component causes a much larger error than neglecting a horizontal component of the same magnitude. A neglected vertical wind of 100 ft/sec would cause a maximum error of about 10% throughout the range of the experiment, whereas neglecting a similar horizontal wind would cause a 1% error. No measurements of vertical winds in the altitude range of the experiment are known to the authors.

2. Velocity and Acceleration

Factors to be considered in evaluating the accuracy of the DOVAP velocities and accelerations are the following:

(1) Cycles per half-second are counted to the nearest 0.1 cy. Thus, there is a least-count error.

(2) False cycle counts due to antenna spin are corrected for only approximately. A residual spin error remains.

(3) Noise in the transmitters and receivers may introduce random errors in the cycle counts.

Patton[11] has estimated the maximum errors due to least-count errors in individual vertical-velocity and vertical-acceleration data points for a nonspinning missile with a trajectory similar to the sphere trajectory. The values are 5.6 ft/sec and 1.5 ft/sec², respectively. If these maximum errors were obtained in the sphere flights, the width of the band of scatter of the individual vertical-acceleration data points would be twice the maximum error, i.e., 3 ft/sec². Table I shows the actual scatter band widths obtained in the sphere flights.

The increase in scatter band widths of the measured data over the predicted data is presumably due to residual spin and noise errors. The maximum errors for the flights, which are one-half the band width of scatter, are shown in the table. Sample calculations for several assumed probability density functions indicate that the probable error should lie in the range 0.3 to 0.5 times the maximum error. These values are also shown in the table. The value of error in acceleration used in calculating the probable errors in density and temperature for the flights was 1.7 ft/sec². The errors in

TABLE II. Trajectory data and sphere constants for sphere experiments at WSPG, New Mexico.

		SC-23	SC-29	SC-30	SC-31
Date	Day	5-14-52	12-11-52	4-23-53	9-29-53
	Time (MST)	18:16:30	16:46:32	12:32:32	13:49:44
Burnout	Time (sec)	36.3	44.1	45.4	33.5
	Altitude (ft)	70 287	93 738	97 989	80 340
	Velocity (ft/sec)	3408	4003	4383	4651
Peak of trajectory	Time (sec)	141.25	170.75	185.9	99
	Altitude (ft)	243 883	344 770	404 705	190 291
	Velocity (ft/sec)	279	572	359	106
Sphere ejection	Time (sec)	144.0	154.8	166.4	46.19
	Altitude (ft)	243 745	340 699	398 700	132 176
Sphere constants	mg (lb)	48.5	41.44	49.8	20.62
	D (ft)	4.32	3.86	4.05	4.03
	A (ft²)	14.66	11.7	12.88	12.72
Altitude range of data (ft)	Density data	(165–215)10³	(115–243)10³	(120–268)10³	(106–174)10³
	Temperature data	(165–170)10³	(115–195)10³	(120–213)10³	(106–125)10³

[11] R. B. Patton, Jr., "Accuracy of DOVAP velocity and vertical acceleration for certain selected points," Ballistic Research Laboratories, Report BRL-TN-292 (1950).

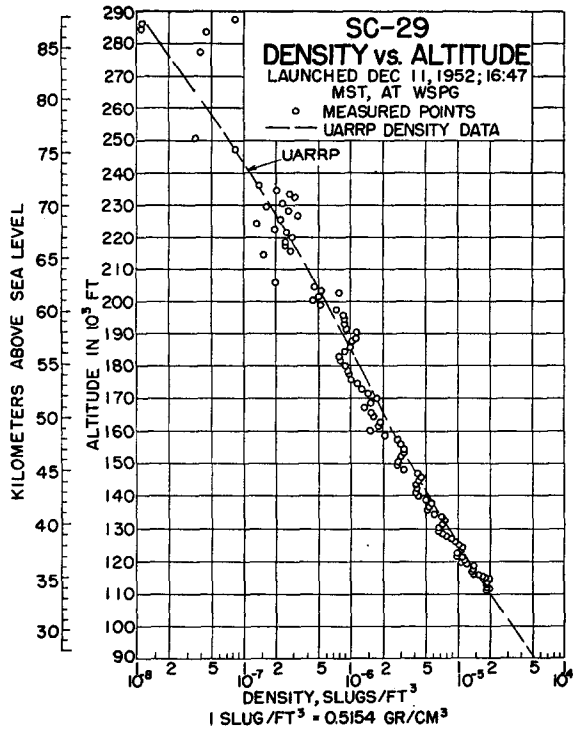

FIG. 4. Density data *vs* altitude above White Sands Proving Ground, New Mexico, obtained from drag-acceleration data of sphere flown on Aerobee SC-29.

DOVAP velocities are also larger than Patton predicted. However, being less than 1%, they are neglected.

3. Drag Coefficient

For most of the altitude range of the experiment where $M>1$ and $\mathrm{Re}>400$, the maximum error in drag coefficient is estimated to be less than 2%. At high altitudes where $M>2$ and $\mathrm{Re}<400$, the error in drag coefficient may be as high as 5%.

4. $T(0)$ and $I(h)$

It was noted above that an error in assumed $T(0)$ for use in Eq. (16) would cause an error in the top 45 000 ft of calculated temperatures. Accordingly, temperature results are presented starting 45 000 ft below the density results, and the error due to $T(0)$ is negligible. The error in the integral $I(h)$ can be shown to be less than the error in $\rho(h)$, the density at the same altitude.

5. Net Error

The individual probable errors are combined according to error theory. Thus, if

$$F=F(x,y,\cdots), \tag{20}$$

and P_x, P_y, $\cdots$ are independent probable errors in x, y, $\cdots$, then the error in F is

$$P_F^2=\left(\frac{\partial F}{\partial x}\right)^2 P_x+\left(\frac{\partial F}{\partial y}\right)^2 P_y+\cdots. \tag{21}$$

Average densities and temperatures were taken over 2- and 4-km intervals. The probable error of the average is given by

$$\bar{P}_F=\frac{P_F}{(n)^{\frac{1}{2}}}, \tag{22}$$

where P_F is the probable error in the individual points and n is the number of points averaged. The values of probable errors shown in Fig. 6 were obtained in this way.

VI. RESULTS

The experiment was flown four times in Aerobee rockets launched at White Sands. None of the flights was perfect, but valid and useful densities and temperatures were obtained from all.

On SC-23, the sphere was ejected near peak. It inflated properly but had a slow leak. The internal pressure record (by DOVAP telemeter) indicated suitable inflation down to 165 000 ft MSL, then collapse.

On SC-29, the sphere was ejected somewhat before peak. It inflated properly but leaked slowly, collapsing at 115 000 ft MSL.

SC-30 ejection also occurred before peak. The sphere inflated properly, and apparently did not leak. During the sphere drop, power to the recorders for

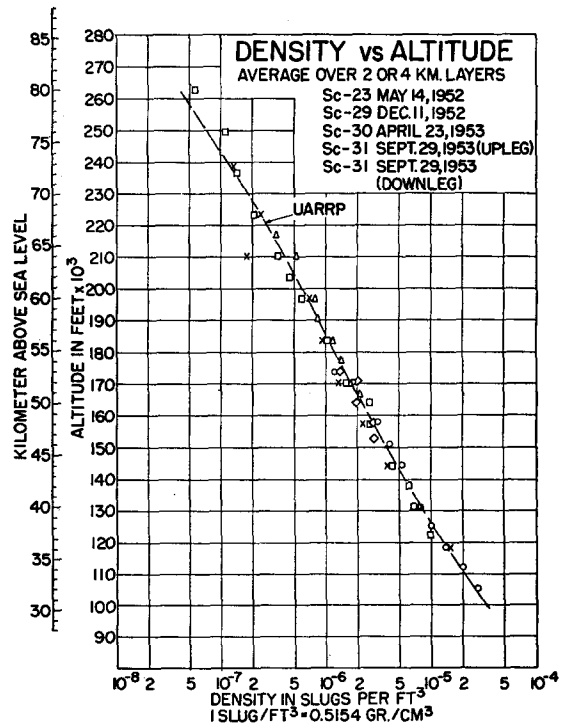

FIG. 5. Average densities *vs* altitude above White Sands Proving Ground, New Mexico, obtained from the data of SC-23 and SC-31 by averaging over 2-km altitude intervals, and from the data of SC-29 and SC-30 by averaging over 4-km altitude intervals. The Rocket Panel, UARRP, data (reference 10) are shown for comparison.

all but two of the DOVAP receivers failed. The trajectory solution for this part of the flight was obtained from the data of the two stations, however, by establishing the vertical plane of the trajectory from the early part of the flight when all stations were operating.

On SC-31, the rocket experienced large yaw angles just before burn-out. Shortly after burn-out, the sphere was ejected prematurely. It inflated peoperly and did not leak. However, due to its large drag, the peak altitude was low.

Table II summarizes the essential features of the four flights. Figure 4 is a plot of the density for each data point of SC-29 together with the Rocket Panel[10] densities for comparison. Figures 5 and 6 contain densities and temperatures, respectively, smoothed by taking averages over suitable layers. The layers are of constant altitude in a given flight, and were chosen so that no average was taken over fewer than 6 points. They are 2 km high for SC-23 and SC-31, and 4 km high for SC-29 and SC-30. The probable errors in the average temperatures, estimated according to Sec. V, are indicated in Fig. 6. Probable errors are not indicated for densities in Fig. 5 because those of adjacent data points would overlap. The probable error (percent) at a given altitude for a given rocket flight is about one-half of the probable error (percent) in the corresponding temperature. The Rocket Panel (UARRP) results are shown for comparison.

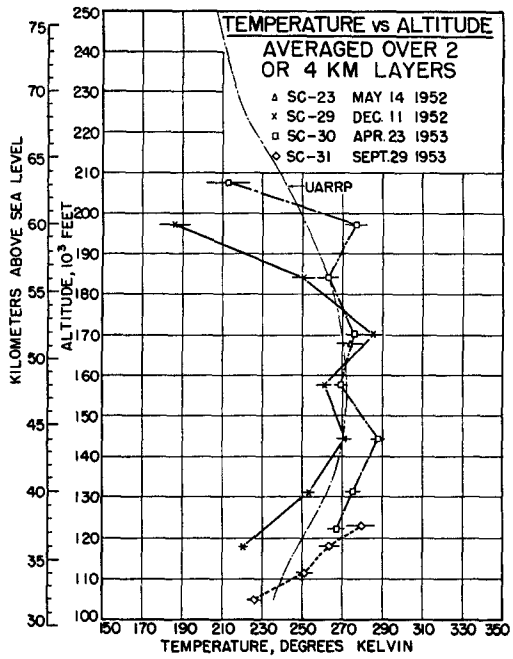

FIG. 6. Average temperatures *vs* altitude above White Sands Proving Groung, New Mexico. The averages have been taken over 2-km altitude intervals for SC-23 and SC-31, and over 4-km altitude intervals for SC-29 and SC-30.

VII. CONCLUSIONS

In summary, it can be said that the experiments operated successfully. The results show good agreement with the Rocket Panel data so that the experiment could be used with confidence to make measurements at places other than White Sands Proving Ground. A synoptic survey of upper-air densities and temperatures could be made. The errors of the DOVAP tracking system were larger than anticipated because of the spin of the transponder antenna. It is felt that techniques can be developed to reduce these errors.